absorption correction was applied by use of psi scan data and programs PSI and EAC.[10]

Solution and Refinement of the Structure. The structure was solved by conventional heavy-atom techniques. The Rh and I atoms were located by Patterson syntheses. Full-matrix least-squares refinement and difference Fourier calculations were used to locate all remaining non-hydrogen atoms. The atomic scattering factors were taken from the usual tabulation,[11] and the effects of anomalous dispersion were included in F_c by using Cromer and Ibers'[12] values of $\Delta f'$ and $\Delta f''$. Tables of observed and calculated structure factor amplitudes are available.[13] Hydrogen atom positions were calculated (C–H distance set at 0.95 Å) for all phenyl ring hydrogen atoms and were included in structure factor calculations but were not refined.

The methyl hydrogen atom positions were located by difference Fourier analysis and were found to be rotationally disordered about the crystallographic twofold axis that contains Rh and C. The final model included six methyl hydrogen positions.

The final difference Fourier map did not reveal chemically significant residual electron density. The final positional and thermal parameters of the refined atoms appear in Tables S1–S3.[13] The labeling scheme is presented in Figure 1.

Acknowledgment. We are grateful to the staff of the 3M Analytical and Properties Research Laboratory for spectroscopic and analytical data. The National Science Foundation is acknowledged for partial support of the X-ray diffraction and structure-solving equipment at the University of Minnesota (Grant CHE77-28505). L.H.P. also acknowledges support by the National Science Foundation (Grant CHE81-08490) of his contribution to this research.

Registry No. **1**, 47829-28-7; **2a**, 89579-39-5; **2b**, 89617-65-2; **3**, 89579-40-8; **4**, 21006-49-5; **5**, 89579-41-9; **6**, 89596-64-5; **7**, 89579-42-0; **8**, 89579-43-1; **9**, 89579-44-2; **10**, 89617-66-3; $(Ph_3P_3Rh^3HC(SO_2CF_3)_2$, 88825-75-6; CH_3I, 74-88-4; t-C_4H_9NC, 7188-38-7; SO_2, 7446-09-5; $(CH_3O)_3P$, 121-45-9; $(CH_3)_3P$, 594-09-2; C_5H_5N, 110-86-1; CO, 630-08-0.

Supplementary Material Available: Tables of positional and thermal parameters, calculated hydrogen positional parameters, and observed and calculated structure factors and an ORTEP stereoview (19 pages). Ordering information is given on any current masthead page.

(11) Cromer, D. T.; Waber, J. T. "International Tables for X-Ray Crystallography"; Kynoch Press: Birmingham, England, 1974; Vol. IV, Table 2.2.4. Cromer, D. T. *Ibid.*; Table 2.3.1.
(12) Cromer, D. T.; Ibers J. A., in ref 11.
(13) See paragraph at end of paper regarding supplementary material.

Cryochemical Studies. 11. ESR Studies of the Reaction of Group 1B Metal Atoms with Some Mono- and Disubstituted Acetylenes in a Rotating Cryostat[1]

J. A. Howard,* R. Sutcliffe,[2] and J. S. Tse

National Research Council of Canada, Ottawa, Ontario, Canada K1A OR9

B. Mile*

Department of Chemistry and Biochemistry, Liverpool Polytechnic, Liverpool, England L3 3AF

Received November 1, 1983

Group 1B metal atoms have been deposited into inert hydrocarbon matrices with a variety of mono- and disubstituted alkynes at 77 K in a rotating cryostat, and their electron spin resonance spectra have been examined. The spectra show that the metal atoms react with the alkynes to give a variety of metal atom mono- and diligand complexes, ML and ML_2, and cis and trans organometallic vinyls. The ESR parameters for the complexes given by substituted alkynes are very similar to those for the prototype complexes $Cu[C_2H_2]$ and $Cu[C_2H_2]_2$ which suggests similar bonding and singly occupied molecular orbitals for all the species. Ab initio calculations have been performed on $Cu[C_2H_2]$ and $Cu[C_2H_2]_2$ and support the Dewar–Chatt–Duncanson model of metal–acetylene bonding. Metal and hydrogen hyperfine interactions for the organometallic vinyls show small differences depending on the nature of the alkyne.

Introduction

Several recent low-temperature (4–77 K) matrix isolation electron spin resonance spectroscopic (ESR) studies have shown that Cu atoms react with acetylene to give the mono- and diligand complexes $Cu[C_2H_2]$ and $Cu[C_2H_2]_2$,[3,4] that Ag atoms and acetylene give pseudocomplexes with one, two, three, and more than three ligands, $Ag\cdots(C_2H_2)$, $Ag\cdots(C_2H_2)_2$, and $Ag\cdots(C_2H_2)_{n\geq 3}$,[3] and the β-silver vinyl $AgCH{=}\dot{C}H$,[3,4] and that gold atoms and acetylene give the monoligand complex $Au[C_2H_2]$[5] and the vinyl and vinylidene radicals $AuCH{=}\dot{C}H$ and $Au\dot{C}{=}CH_2$.[4,5] Reaction of all three group 1B metal atoms with phenylacetylene give β-substituted α-styryls.[4]

Apart from our work on phenylacetylene very little is known about the paramagnetic properties of the species formed by reaction of metal atoms with substituted acetylenes. We, therefore, report here the results of a study of the reaction of a series of mono- and disubstituted acetylenes with the group 1B metal atoms Cu, Ag, and Au

(1) (a) Issued as NRCC No. 23105. (b) Part 10. See: Howard, J. A.; Sutcliffe, R.; Mile, B. *J. Phys. Chem.* **1984**, *88*, 171–174.
(2) NRCC Research Associate.
(3) Kasai, P. H.; McLeod, D., Jr.; Watanabe, T. *J. Am. Chem. Soc.* **1980**, *102*, 179–190.
(4) Chenier, J. H. B.; Howard, J. A.; Mile, B.; Sutcliffe, R. *J. Am. Chem. Soc.* **1983**, *105*, 788–791.
(5) Kasai, P. H. *J. Am. Chem. Soc.* **1983**, *105*, 6704–6710.

0276-7333/84/2303-0859$01.50/0 Published 1984 by the American Chemical Society

in a rotating cryostat at 77 K. This paper also reports the results of ab initio calculations on $Cu[C_2H_2]$ and $Cu[C_2H_2]_2$.

Experimental Section

Materials. Methylacetylene, *tert*-butylacetylene, (trifluoromethyl)acetylene, dimethylacetylene, di-*tert*-butylacetylene, diphenylacetylene, and bis(trifluoromethyl)acetylene were used after degassing and distillation. ^{107}Ag and ^{63}CuO were obtained from Oak Ridge National Laboratory, Oak Ridge, TN. ^{63}CuO was reduced to ^{63}Cu with hydrogen at 500 °C. Pure Au and natural Ag and Cu were kindly provided by Dr. C. M. Hurd (NRC, Ottawa, Ontario).

Cryostat. The rotating cryostat and the method used to vaporize group 1B metals and investigate their reaction with organic compounds in an inert matrix at 77 K have been described elsewhere.[6-8]

ESR Measurements. ESR spectra were recorded at 77 K on a Varian E-4 spectrometer. Spectra at higher temperatures were obtained with the aid of a variable-temperature accessory. The microwave frequency was measured with a Systron-Donner Model 6057 frequency counter and the magnetic field with a Varian E-500 NMR gaussmeter.

Computational Details. Ab initio molecular orbital calculations were carried out with the PSHONDO program package[9] employing the pseudopotential method proposed by Durand and Barthelat.[10] The copper effective core potential parameters were derived from an approximate relativistic calculation of the copper atom.[11] The valence basis set was of triple-ζ quality. For the copper atom we used the [4s3p6d/3s2p3d] basis set obtained by optimizing the valence energy of the $^2S(4s^13d^{10})$ state.[12] For the carbon and hydrogen atoms Dunnings'[13] [9s5p/5s3p] and [4s/3s] base sets were used. The open-shell SCF energies were calculated by the Nesbet effective operator.[14] The acetylene ligand was assumed to be linear, with $r(C{\equiv}C) = 1.205$ Å and $r(C{-}H) = 1.06$ Å. For both $Cu[C_2H_2]$ and $Cu[C_2H_2]_2$, the metal–acetylene distance was set at 2.0 Å and no attempt was made to optimize the geometry.

Results

$CH_3C{\equiv}CH$. ^{63}Cu and $CH_3C{\equiv}CH$ gave a complex ESR spectrum consisting of isotropic lines from the mono(alkyne) π complex $Cu[CH_3C{\equiv}CH]$ ($a_{63} = 1338$ G, $g = 2.0056$), the bis(alkyne) π complex $Cu[CH_3C{\equiv}CH]_2$ ($A_\parallel(Cu) \approx 0$ G, $A_\perp(Cu) \approx 65$ G, $A_\parallel(2H) \approx A_\perp(2H) \approx 30$ G, $g_\parallel \approx g_\perp \approx 2.000$), propargyl $HC{\equiv}\dot{C}CH_2$ ($a_H(1) = 14.8$ G, $a_H(2) = 18.5$ G, $g = 2.0025$), and a copper-substituted vinyl $CuCH{=}\dot{C}CH_3$. The copper and hydrogen hyperfine coupling constants for $CuCH{=}\dot{C}CH_3$ could not be determined because only the $|M_I(Cu), M_I(H)\} = |^3/_2, {}^1/_2\}$ and $|{-}^3/_2, {-}^1/_2\}$ transitions were not masked by the more intense lines from $Cu[CH_3C{\equiv}CH]_2$. We could, however, estimate that $3a_{63} + a_H = 525$ G.

^{107}Ag and $CH_3{\equiv}CH$ in adamantane gave at least five doublets with large Ag coupling constants: (I) $a_{107} = -645.5$ G, $g = 1.996$; (II) $a_{107} = -615.2$ G, $g = 2.0011$; (III) $a_{107} = -593.7$ G, $g = 2.0009$; (IV) $a_{107} = -559.5$ G; $g = 1.9999$; (V) $a_{107} = -535.2$ G, $g = 1.9996$. Species I, II, and III have Ag hyperfine interactions similar to the values for Ag atoms isolated in two magnetically nonequivalent sites in adamantane.[8] It would, however, appear that we detected an extra site in the present system. Species IV and V have values of a_{Ag} similar to the values for the monoligand complexes $Ag[C_2H_4]$[3] and $Ag[C_6H_6]$,[4] and we tentatively suggest that they can be assigned to the monoligand complex $Ag[CH_3C{\equiv}CH]$ in two sites.

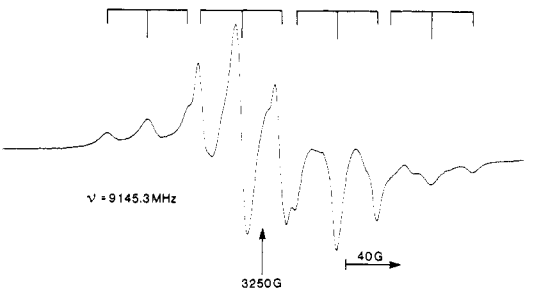

Figure 1. The central portion of the ESR spectrum from adamantane containing ^{63}Cu and *tert*-butylacetylene at 77 K.

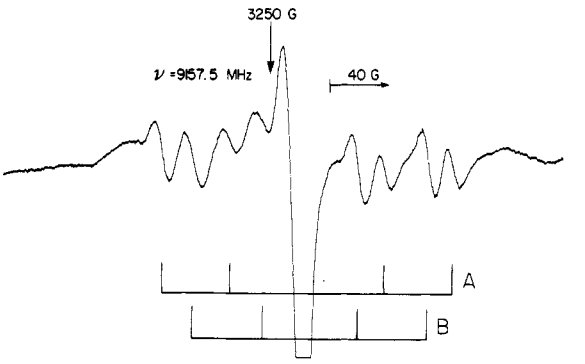

Figure 2. The ESR spectrum from adamantane containing ^{107}Ag and *tert*-butylacetylene at 77 K.

In the center of the spectrum several isotropic lines were evident which could be assigned to $AgCH{=}\dot{C}CH_3$ and $CH{\equiv}C\dot{C}H_2$. Only the high field 1:3:3:1 quartet from $AgCH{=}\dot{C}CH_3$ was well resolved. Computer simulation of the spectrum gave $a_{107}(1) = -160$ G, $a_H(1) = 40$ G, $a_H(3) = 13$ G, and $g = 2.000$.

Au atoms and $CH_3C{\equiv}CH$ in adamantane gave two major quartets (I and III) and two much less intense quartets with large Au coupling constants. The parameters for these four species are as follows: (I) $a_{Au} = 1045.3$ G, $g = 2.0025$; (II) $a_{Au} = 1018.8$ G, $g = 2.0018$, (III) $a_{Au} = 1035.7$ G, $g = 2.0038$; (IV) $a_{Au} = 1027.1$ G, $g = 2.0034$. Interestingly the relative intensities of the species I, II, and III were quite different to that found in adamantane alone.[8] A broad ($\Delta H_{pp} \approx 40$ G) slightly anisotropic quartet was also evident with $a_{Au} = 603.5$ G and $g = 1.9802$, and the magnitude of the hyperfine interaction and g factor suggests that it is the Au mono(alkyne) complex $Au[CH_3C{\equiv}CH]$.[5]

The central region was dominated by the isotropic spectrum of propargyl, $a_H(1) = 14.8$ G, $a_H(2) = 18.5$ G, and $g = 2.0025$, produced by abstraction of a primary hydrogen from the methyl group by a Au atom.

The adduct $AuCH{=}\dot{C}CH_3$ was definitely formed in this system. The signal was, however, too weak, unstable, and complex for a satisfactory analysis to be accomplished.

$(CH_3)_3CC{\equiv}CH$. ^{63}Cu and $(CH_3)_3CC{\equiv}CH$ gave the anisotropic spectrum shown in Figure 1 which can be analyzed in terms of an overlapping quartet of triplets with $A_\parallel(Cu) \approx 0$ G, $A_\perp(Cu) \approx 68$ G, $A_\parallel(H) = A_\perp(H) \approx 28$ G, $g_\parallel = 1.996$, and $g_\perp = 2.003$ and is assigned to $Cu[(CH_3)_3CC{\equiv}CH]_2$. There was no evidence for lines from the mono(alkyne) complex $Cu[(CH_3)_3CC{\equiv}CH]$, the organo-

(6) Bennett, J. E.; Thomas, A. *Proc. R. Soc. London, Ser. A* **1964**, *280*, 123–138.
(7) Bennett, J. E.; Mile, B.; Thomas, A.; Ward, B. *Adv. Phys. Org. Chem.* **1970**, *8*, 1.
(8) Buck, A. J.; Mile, B.; Howard, J. A. *J. Am. Chem. Soc.* **1983**, *105*, 3381–3387.
(9) Ruiz, M. E.; Daudey, J. P.; Novaro, O. *Mol. Phys.* **1982**, *46*, 853–862.
(10) Durand, Ph.; Barthelat, J. C. *Theor. Chim. Acta* **1975**, *38*, 283–302.
(11) Barthelat, J. C.; Pélissier, M.; Durand, Ph. *Phys. Rev. A* **1980**, *21*, 1773–1785.
(12) Pélissier, M. *J. Chem. Phys.* **1981**, *75*, 775–780.
(13) Dunning, T. H., Jr. *J. Chem. Phys.* **1970**, *53*, 2823–2833.
(14) Nesbet, R. K. *Rev. Mod. Phys.* **1963**, *35*, 552–557.

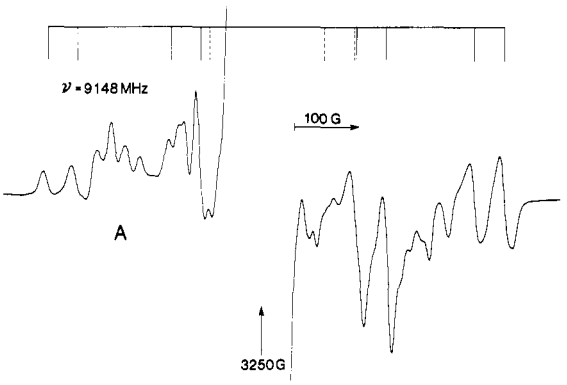

Figure 3. The central portion of the ESR spectrum from adamantane containing Au and *tert*-butylacetylene at 77 K.

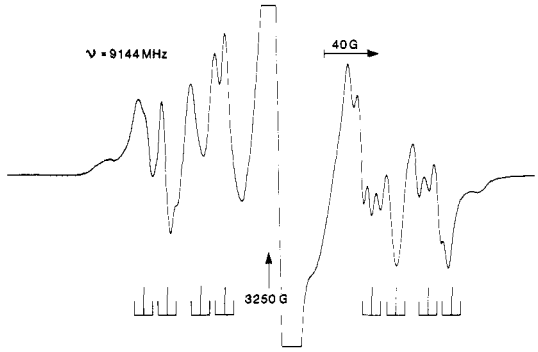

Figure 4. The ESR spectrum from adamantane containing ^{107}Ag and (trifluoromethyl)acetylene at 77 K.

copper vinyl CuCH=ĊC$(CH_3)_3$, or isolated Cu atoms.

^{107}Ag and low concentrations of $(CH_3)_3CC{\equiv}CH$ in adamantane gave a spectrum consisting of weak lines from isolated Ag atoms, an intense isotropic double of doublets with $a_{107}(1) = -149.6$ G, $a_H(1) = 46$ G, and $g = 1.9996$, and an intense anisotropic central feature. The doublet of doublets is assigned to AgCH=ĊC$(CH_3)_3$, and this species decayed fairly rapidly at 118 K. Ag atoms and higher concentrations of $(CH_3)_3CC{\equiv}CH$ gave *two* isotropic doublets of doublets with distinct Ag hyperfine coupling constants ($a_{107} = -149.6$ G and -110.5 G) and similar H coupling constants ($a_H = 46$ and 47.7 G); see Figure 2. Two stereoisomeric forms of AgCH=ĊC$(CH_3)_3$ are apparently formed at the higher alkyne concentration. Annealing experiments indicated that the species with the larger silver hyperfine coupling constant decayed more rapidly than the species with the lower silver coupling constant. There was no evidence for cis–trans isomerization during these annealing experiments, and radical decays were irreversible. There were no lines in the spectrum of Ag and $(CH_3)_3CC{\equiv}CH$ which could be assigned to the mono- and diligand complexes $Ag[(CH_3)_3CC{\equiv}CH]_n$ where $n = 1$ or 2.

Au and $(CH_3)_3CC{\equiv}CH$ in adamantane gave Au atoms in two major trapping sites ($a_{Au}^{I} = 1045.3$ G, $g = 2.0025$; $a_{Au}^{III} = 1018.8$ G, $g = 2.0018$) and two minor trapping sites ($a_{Au}^{II} = 1035.7$ G, $g = 2.0038$; $a_{Au}^{IV} = 1027$ G, $g = 2.0034$), a broad anisotropic quartet with $A_{\parallel} = 620$ G, $A_{\perp} = 640$ G, $g_{\parallel} = 2.000$, and $g_{\perp} = 1.987$, a quartet of doublets, and an intense anisotropic species at the center of the spectrum. The central feature of this spectrum is shown in Figure 3. The stick diagram indicates the field positions of the spectrum from a species that is almost certainly AuCH=ĊC$(CH_3)_3$. Analysis of this spectrum using the $M_I = \pm^3/_2$ transitions gave $a_{Au}(1) = 218$ G, $a_H(1) = 45$ G, and $g = 1.9931$. The positions of the $M_I = \pm^1/_2$ lines predicted from this analysis are shown as broken lines in Figure 3, and it can be seen that the $M_I = -^1/_2$ doublet is shifted ~50 G upfield and the $M_I = {}^1/_2$ lines are shifted ~15 G downfield. The group of lines labeled A are similar to the low field features in the ESR spectra from $Ag[C_2H_4]_2$[3] and $Au[C_2H_4]_2$[5] and are tentatively assigned to the diligand complex $Au[(CH_3)_3CC{\equiv}CH]_2$. Interestingly Kasai[5] did not observe analogous features in the spectrum from Au and C_2H_2.

When the sample was heated to 193 K, all the paramagnetic Au species had decayed and we were left with an almost isotropic doublet with $a_H = 54$ G which was almost certainly a polymeric radical RCH=ĊC$(CH_3)_3$ where R is AuCH=CC$(CH_3)_3$[CH=CC$(CH_3)_3]_n$.

$CF_3C{\equiv}CH$. ^{63}Cu and $CF_3C{\equiv}CH$ gave a broad anisotropic spectrum centered about $g \approx 2$ which could be analyzed in terms of an overlapping quartet of triplets. By analogy with other anisotropic spectra from Cu atoms and alkynes this spectrum can be assigned to $Cu[CF_3C{\equiv}CH]_2$ with $A_{\parallel}(Cu) \approx 0$ G, $A_{\perp}(Cu) \approx 70$ G, $A_{\parallel}(2H) = A_{\perp}(2H) \approx 30$ G, and $g_{\parallel} \approx g_{\perp} \approx 1.992$. In addition to this spectrum there was evidence for the highest and lowest field lines of the spectrum from CuCH=ĊCF_3 with $3a_{Cu} + a_H = 464$ G and $g = 2.001$. There was no evidence for lines from Cu atoms or $Cu[CF_3C{\equiv}CH]$.

Ag and $CF_3C{\equiv}CH$ gave weak lines from Ag atoms and an intense central feature shown in Figure 4. Part of the central feature can be analyzed in terms of a doublet of doublets of triplets with $a_{107}(1) = -164$ G, $a_H(1) = 41$ G, $a_F(1) = 17$ G, and $a_F(2) = 6.5$ G. These parameters are assigned to AgCH=ĊCF_3 in which the CF_3 group is not freely rotating.

Au and $CF_3C{\equiv}CH$ gave a broad ($\Delta H_{pp} \approx 80$ G) anisotropic spectrum centered at $g \approx 2$ flanked by very weak isotropic lines from a gold-containing species with $a_{Au}(1) = 274$ G, $a_H(1) = 35$ G, and $a_F(1) = 15$ G. At temperatures >77 K the central feature resolved into a doublet of triplets which are assigned to CH=CĊF_2 ($a_H(1) = 10$ G, $a_F(2) = 25$ G).

$CH_3C{\equiv}CCH_3$. ^{63}Cu and $CH_3C{\equiv}CCH_3$ gave a weak signal from isolated ^{63}Cu atoms, two quartets with $a_{Cu}^{I} = 1333$ G, $g = 2.0007$, $a_{Cu}^{II} = 1357$ G, and $g = 1.9988$ which are assigned to $Cu[CH_3C{\equiv}CCH_3]$ in two sites and a strong anisotropic spectrum with $A_{\parallel}(Cu) \approx 0$, $A_{\perp}(Cu) \approx 70$ G, and $g_{\parallel} \approx 2.000$ which is assigned to $Cu[CH_3C{\equiv}CCH_3]_2$. There were also isotropic lines in the center of the spectrum which have been assigned to $CH_3C{\equiv}CĊH_2$ ($a_H(2) = 18.5$ G, $a_H(3) = 12.6$ G, $g = 2.0027$). The copper adduct CuC(CH_3)=ĊCH_3 was not detected.

^{107}Ag and $CH_3C{\equiv}CCH_3$ gave Ag atoms, $Ag[CH_3C{\equiv}CCH_3]$ ($a_{107} = -556.6$ G, $g = 2.002$), AgC(CH_3)=ĊCH_3, and $CH_3C{\equiv}CĊH_2$. The signal from AgC(CH_3)=ĊCH_3 was very weak and decayed rapidly at 103 K and was much less stable than $Ag[CH_3C{\equiv}CCH_3]$.

Au and $CH_3C{\equiv}CCH_3$ gave isolated Au atoms, a broad anisotropic quartet with $A_{\parallel} = 621$ G, $A_{\perp} = 638$ G, $g_{\parallel} = 2.000$, and $g_{\perp} = 1.971$ which is assigned to $Au[CH_3C{\equiv}CCH_3]$, a very weak adduct with $a_{Au} \approx 187$ G and $g = 1.986$ and an intense isotropic spectrum from $CH_3C{\equiv}CĊH_2$.

$(CH_3)_3CC{\equiv}CC(CH_3)_3$. ^{63}Cu and di-*tert*-butylacetylene gave three major paramagnetic species in adamantane: $Cu[(CH_3)_3CC{\equiv}CC(CH_3)_3]$ ($a_{63} = 1285$ G, $g = 1.9932$) with line widths which decreased with increasing field from ~160 G for the lowest field line to ~70 G for the highest field line; $Cu[(CH_3)_3CC{\equiv}CC(CH_3)_3]_2$ with $A_{\parallel}(Cu) \approx 0$ G, $A_{\perp}(Cu) \approx 65$ G, and $g_{\parallel} = g_{\perp} = 2.000$ and CuC$((CH_3)_3C)$-=ĊC$(CH_3)_3$ with $a_{Cu} = 397.3$ G and $g = 2.0007$. This vinyl radical exhibited a marked M_I effect on the line width with ΔH_{pp} following the order $+^3/_2 > {}^1/_2 >> -^1/_2 << -^3/_2$.

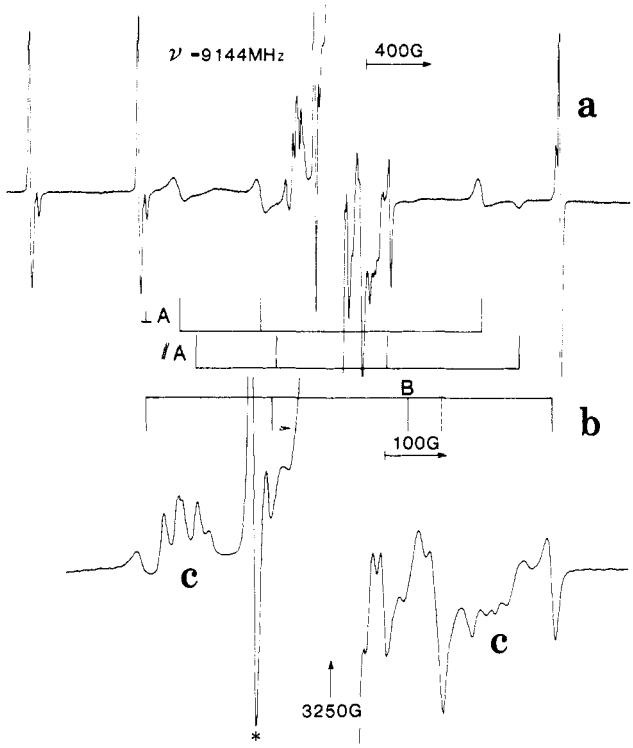

Figure 5. The ESR spectrum from adamantane containing Au and di-*tert*-butylacetylene at 77 K.

^{107}Ag and $(CH_3)_3CC{\equiv}CC(CH_3)_3$ gave two doublets from isolated ^{107}Ag atoms, an intense doublet from Ag[$(CH_3)_3CC{\equiv}CC(CH_3)_3$] with a_{107} = −554 G and g = 1.9992 and two weaker doublets from two adducts with a_{107} = −102 G, g = 2.0004, and a_{107} = −154 G, g = 2.004.

Au and $(CH_3)_3CC{\equiv}C(CH_3)_3$ gave the ESR spectrum shown in Figure 5. The upper spectrum consists of quartets from Au atoms in two sites (a_{Au} = 1046 G, g = 2.0017, a_{Au} = 1028 G, g = 2.0022), a broad anisotropic quartet labeled A ($\Delta H_{pp} \approx 73$ G) with $A_\parallel$ = 659 G, $g_\parallel$ = 1.8859, $A_\perp \approx 612$ G, and $g_\perp$ = 1.976 and a central feature consisting of isotropic and anisotropic lines. The isotropic and dipolar contributions of the Au hyperfine interaction (hfi) for A, calculated from $A_\parallel = A_{iso} + 2A_{dip}$ and $A_\perp = A_{iso} - A_{dip}$, are A_{iso} = 621 G and A_{dip} = 14 G. The percentage unpaired 6s spin population in the SOMO of A is ~60%, and we conclude that this species is the monoligand complex Au[$(CH_3)_3CC{\equiv}CC(CH_3)_3$]. The central feature of the spectrum from Au and $(CH_3)_3CC{\equiv}CC(CH_3)_3$ is shown in expanded scale in Figure 5b. The $M_I = \pm^3/_2$ components of a quartet are resolved and the field positions of these lines gave $a_{Au}(1)$ = 204 G and g = 2.000. The $M_I = \pm^1/_2$ lines predicted from this analysis are shown in the stick diagram in Figure 5b. The Au hfi of this species is similar but not exactly equal to a_{Au} for $AuCH{=}\dot{C}C(CH_3)_3$, and we conclude that it is $AuC((CH_3)_3C){=}\dot{C}C(CH_3)_3$. When the sample was warmed to 168 K, the Au atoms, Au[$(CH_3)_3CC{\equiv}CC(CH_3)_3$], and $AuCC(CH_3)_3{=}\dot{C}C(CH_3)_3$ decayed irreversibly and the anisotropic feature at the center remained. The low and high field features of this species are labeled C in Figure 5b and are similar to the analogous features in the spectra from Ag[C_2H_4]$_2$[3] and Au[C_2H_4]$_2$[5] and are tentatively assigned to the diligand complex Au[$(CH_3)_3CC{\equiv}CC(CH_3)_3$]$_2$ with g_1 = 1.884, g_2 = 2.009, g_3 = 2.157, A_1 = 27.5 G, A_2 = ~0, and A_3 = 20 G.

$CF_3C{\equiv}CCF_3$. All the group 1B metal atoms reacted with $CF_3C{\equiv}CCF_3$ to give composite spectra which were almost impossible to deconvolute. The broad and overlapping lines were probably associated with unresolved fluorine hyperfine interactions.

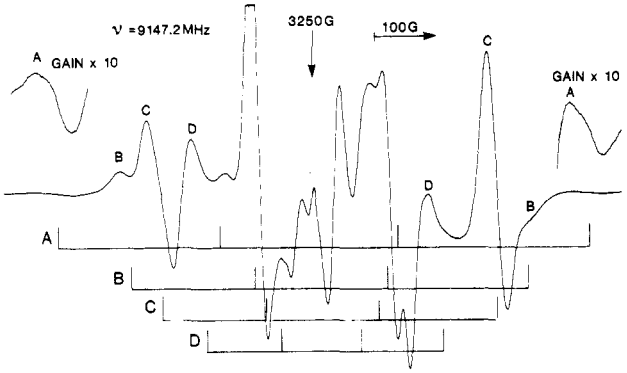

Figure 6. The ESR spectrum from adamantane containing Au and diphenylacetylene at 77 K.

$C_6H_5C{\equiv}CC_6H_5$. ^{63}Cu atoms and diphenylacetylene gave a strong central feature which is assigned to Cu[$C_6H_5C{\equiv}CC_6H_5$]$_2$ with $A_\perp$(Cu) ≈ 67 G, $A_\parallel$(Cu) ≈ 0 G, and $g_\perp \approx g_\parallel \approx 2.000$. In addition to this anisotropic spectrum two less intense quartets were apparent with $a_{Cu}(1)$ = 339 G, g = 2.0012, and $a_{Cu}(1)$ = 257 G, g = 2.005, which are assigned to *trans*- and *cis*-$CuC(C_6H_5){=}\dot{C}C_6H_5$. The ESR and NMR lines from Cu atoms could also be identified in the spectrum, but there was no evidence of a spectrum from the monoligand complex Cu[$C_6H_5C{\equiv}CC_6H_5$]. When the sample was warmed, the spectra from the two vinyls sharpened and the cis isomer decayed before the trans isomer. Both vinyls were, however, less stable than Cu[$C_6H_5C{\equiv}CC_6H_5$]$_2$.

^{107}Ag and diphenylacetylene gave isolated Ag atoms (a_{107} = −601.4 G, g = 2.0008) and one vinyl radical $AgC(C_6H_5) = \dot{C}C_6H_5$ ($a_{107}(1)$ = −108.3 G, g = 2.004). There was also a weak doublet with a_{107} = −404.3 G and g = 1.9960 which decayed slowly when the sample was warmed to 100 K.

Au atoms and diphenylacetylene gave a complex spectrum, the central portion of which is shown in Figure 6. Treatment of the lines labeled A as $\pm^1/_2$ lines of a Au monoligand complex gave a_{Au} = 921 G and g = 1.7603, with lines at 2136, 2815, 3750, and 4941 G. Although there was possibly a weak absorption at 2150 G, the line intensities and g factor were not consistent with a monoligand complex. Treatment of these lines as the $M_I = \pm^3/_2$ lines of a vinyl gave a_{Au} = 283 G and g = 1.989 with predicted lines at 2842, 3101, 3385, and 3694 G. However, the line intensities and behavior on annealing suggested that these inner lines may be the result of a further species A′ with $a_{Au} \approx 103$ G. Spectral calculation and simulation suggest three additional species labeled B, C, and D with the following parameters: B, a_{Au} = 208 G, g = 2.0071; C, a_{Au} = 179 G, g = 2.0056; D, a_{Au} = 121 G, g = 2.021. There were, however, substantial errors involved in calculating these parameters because of broad and overlapping lines.

Warming the sample to ~100 K caused the species labeled B to decay immediately. All the other species decayed slowly on further warming to ~180 K. Species C was the most stable and D decayed more rapidly than A′, the latter becoming more pronounced on warming. However, it was unclear whether the lines labeled A were still present making analysis of A and A′ lines difficult. As these species disappeared a broad doublet with $a \approx 41$ G and g = 2.000 appeared and remained at high temperatures. This species did not undergo the line width variations observed for the doublets from $(CH_3)CC{\equiv}CH$ on cooling and rewarming.

The spectrum from Au and $C_6H_5C{\equiv}CH$ was less complex than the one that we report here for the Au/$C_6H_5C{\equiv}CC_6H_5$ system, and we identified[4] two vinyls,

Table I. ESR Parameters for Some Group 1B Metal Atom Mono(alkyne) Complexes in Adamantane at 77 K

complex	a_M/G	g factor
$Cu[C_2H_2]$	1479	
	1218	
$Cu[CH_3C{\equiv}CH]$	1338	2.0056
$Cu[CH_3C{\equiv}CCH_3]$	1333	2.0007
	1357	1.9988
$Cu[(CH_3)_3CC{\equiv}CC(CH_3)_3]$	1285	1.9932
$Ag[CH_3C{\equiv}CH]$	−535.2	1.996
	−559.5	2.000
$Ag[CH_3C{\equiv}CCH_3]$	−556.6	2.0002
$Ag[(CH_3)_3CC{\equiv}CC(CH_3)_3]$	−554	1.992
$Ag[C_6H_5C{\equiv}CC_6H_5]$	−404.2	1.9960
$Au[C_2H_2]$[a]	683	1.945
$Au[CH_3C{\equiv}CH]$	603.5	1.9802
$Au[CH_3C{\equiv}CCH_3]$	621	1.9708
	638	1.9802

[a] Reference 5.

trans-$AuCH{=}\dot{C}C_6H_5$ and *cis*-$AuCH{=}\dot{C}C_6H_5$ with a_{Au} = 189.1 and 107 G, respectively. The most abundant species in the present system C has a Au hfi and stability which suggest that it is *trans*-$Au\dot{C}(C_6H_5){=}\dot{C}C_6H_5$. *cis*-$Au\dot{C}(C_6H_5){=}\dot{C}(C_6H_5)$ must also be present in the system and is probably species A′ with $a_{Au} \approx 103$ G. Species A, B, and D are difficult to identify although A has a_{Au} similar to the value for $Au\dot{C}{=}CH_2$ and is possibly the vinylidene radical $Au\dot{C}{=}C(C_6H_5)_2$ formed by rearrangement of $Au\dot{C}(C_6H_5){=}\dot{C}C_6H_5$.

Discussion

Cu, Ag, and Au atoms (M) react with mono- and disubstituted acetylenes (RC≡CH and RC≡CR) to give a variety of mono- and diligand complexes (M[RC≡CH], M[RC≡CR], M[RC≡CH]$_2$, and M[RC≡CR]$_2$) and organometallic vinyls (MCH=CR and MC(R)=CR) with the ESR parameters listed in Tables I–IV.

The monoligand copper complexes that are produced have copper hyperfine interactions and unpaired 4s spin populations similar to those for $Cu[C_2H_2]$.[3] There is, however, no detectable *A* or *g* anisotropy associated with Cu[RC≡CH] and Cu[RC≡CR] whereas the spectrum from $Cu[C_2H_2]$ exhibits measurable *A* and *g* anisotropy.[3] This is probably because the lines from Cu[RC≡CH] and Cu[RC≡CR] are broader than those of $Cu[C_2H_2]$, e.g., ΔH_{pp} for the $M_I = +^3/_2$ lines of $Cu[CH_3C{\equiv}CCH_3]$ and $Cu[(CH_3)_3CC{\equiv}CC(CH_3)_3]$ are ~70 G.

The silver monoalkyne complexes all have about 90% unpaired 5s spin population on the silver nucleus which is similar to the value for $Ag[C_2H_2]$[3] and $Ag[C_6H_6]$.[8] Kasai, McLeod, and Watanabe have suggested that three pseudocomplexes $Ag{\cdots}C_2H_2$, $Ag{\cdots}(C_2H_2)_2$, and $Ag{\cdots}(C_2H_2)_{n\geq 3}$ with ρ_{4s} = 0.97, 0.92, and 0.89, respectively, are formed from Ag and C_2H_2 whereas we have concluded that $Ag[C_6H_6]$ is a genuine monoligand complex. The evidence for one-, two-, and three-ligand pseudocomplexes is based on the dependence of relative spectrum intensity as a function of the ratio of Ag to C_2H_2 whereas our assignment is based on relative complex stability. Since there is no unambigous evidence for either assignment, we prefer to conclude that Ag[RC≡CH] and Ag[RC≡CR] are genuine complexes. The mono(diphenylacetylene)silver complex has less unpaired 5s spin population on the Ag nucleus ($\rho_{5s} \approx 0.67$) probably because the unpaired electron is delocalized onto the two phenyl rings.

Mono(alkyne)gold complexes have unpaired 6s spin populations similar to ρ_{4s} for mono(alkyne)copper complexes.

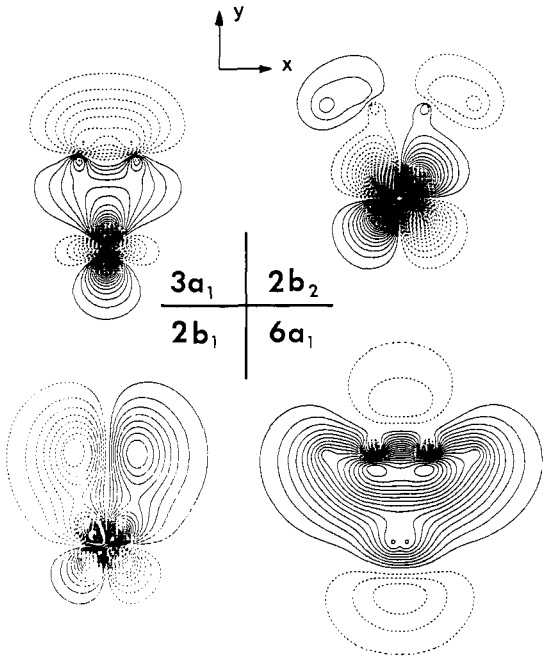

Figure 7. Wave function contour diagrams for the anticipated bonding molecular orbitals of $Cu[C_2H_2]$. Positive and negative wave function contours are indicated by solid and dashed lines, respectively.

The molecular orbital description of bonding for group 1B metal atom mono(substituted acetylene) complexes must be similar to the one for $Cu[C_2H_2]$[3,15] which has been discussed in terms of the Dewar–Chatt–Duncanson model.[16,17] Kasai, McLeod, and Watanabe[3] postulate a strong dative interaction between the Cu d_{xy} orbital and the acetylene π_y^* orbital with the unpaired electron in a nonbonding sp_y-hydridized orbital pointing away from the double bond while Ozin, McIntosh, Power, and Messmer[15] suggest that the main acetylene to metal σ-bonding interaction involves a mixture of the C–C in plane π-bonding orbital and the metal 4s, 4p, and 3d orbitals with some slight back-donation of charge density from the d_{xz} orbital to the out-of-plane C–C π orbital. The large energy difference between the acetylene π_y^* orbitals and the $3d_{xy}$ orbital appears to minimize back-donation into the antibonding orbitals.

An ab initio calculation on $Cu[C_2H_2]$ supports the Dewar–Chatt–Duncanson model of metal–acetylene bonding. The calculation suggests the degree of metal to ligand back-bonding ($2b_2$) is much weaker than the σ interaction between the π orbitals of the acetylene with the metal 3d orbitals as manifested in the $3a_1$, $2b_1$, and $6a_1$ molecular orbitals (Figure 7). The unpaired electron is placed in the $6a_1$ orbital which has ~80% 4s and ~20% $4p_y$ character in a lobe pointing away from the acetylene. The absence of appreciable back-bonding agrees with the Xα–SW calculation,[15] but the two methods differ in the description of the $6a_1$ orbital. The Xα result shows this orbital to be predominantly Cu $3d_z^2$ and 4s in character and antibonding to the acetylene π orbital. Our calculation, however, indicates that it is sp hybridized with a small overlap between the empty Cu $4p_y$ orbital and the π orbital of the acetylene. This large p contribution to the singly occupied molecular orbital (SOMO) is similar to that in $Cu[C_6H_6]$[8] and agrees with Kasai's qualitative formulation of the

(15) Ozin, G. A.; McIntosh, D. F.; Power, W. J.; Messmer, R. P. *Inorg. Chem.* **1981**, *20*, 1782–1792.
(16) Dewar, M. J. S. *Bull Soc. Chim. Fr.* **1951**, *18*, C71–79.
(17) Chatt, J.; Duncanson, L. A. *J. Chem. Soc.* **1953**, 2939–2947.

Table II. ESR Parameters for Some Group 1B Metal Atom Bis(alkyne) Complexes in Adamantane at 77 K

complex	$A_\perp$(Cu)/G	$A_\parallel$(Cu)/G	A(H)/G	g factor
$Cu[C_2H_2]_2$	67 ± 5	~0	29 ± 3	2.0019
$Cu[CH_3C{\equiv}CH]_2$	~65	~0	~30	2.000
$Cu[(CH_3)_3CC{\equiv}CH]_2$	~70	~0	~29	1.995
$Cu[CF_3C{\equiv}CH]_2$	~70	~0	~30	1.992
$Cu[CH_3C{\equiv}CCH_3]_2$	~70	~0		2.000
$Cu[(CH_3)_3CC{\equiv}CC(CH_3)_3]_2$	~70	~0		2.000
$Cu[C_6H_5C{\equiv}CC_6H_5]_2$	~67	~0		2.000

Table III. ESR Parameters for the Adducts Produced from Group 1B Metal Atoms and Some Monosubstituted Acetylenes in Adamantane at 77 K

adduct	a_M/G	a_H/G	g factor
$CuCH{=}\dot{C}H$[a]	191.5	51.0,[b] 27.8[c]	2.002
$CuCH{=}\dot{C}CH_3$	~158[d]	e	2.0023
$CuCH{=}\dot{C}CF_3$	~138[d]	e	2.0013
$CuCH{=}\dot{C}C_6H_5$	133.7	45.1	2.0019
$AgCH{=}\dot{C}H$	−150.5[f]	50.1,[b,f] 28.7[c,f]	1.9988
	−127[g]	50,[b,f] 30[c,f]	2.0028
$AgCH{=}\dot{C}CH_3$	−160	~45	~2.000
cis-$AgCH{=}\dot{C}C(CH_3)_3$	−110.5	47.7	1.9988
trans-$AgCH{=}\dot{C}C(CH_3)_3$	−149.6	46.0	1.9996
$AgCH{=}\dot{C}CF_3$	−164	41	2.000
$AgCH{=}\dot{C}C_6H_5$	−109.6	46.3	2.0014
$AuCH{=}\dot{C}H$[f]	224[f]	41.5,[b,f] 20[c,f]	1.9938
	220[g]	50,[b,g] 25[c,g]	2.002
$AuCH{=}\dot{C}CH_3$	~194	e	~1.983
cis-$AuCH{=}\dot{C}C(CH_3)_3$	160	e	
trans-$AuCH{=}\dot{C}C(CH_3)_3$	218	45	1.9931
cis-$AuCH{=}\dot{C}C_6H_5$	107	e	1.997
trans-$AuCH{=}\dot{C}C_6H_5$	189.1	45.6	1.997

[a] Prepared from photoexcited Cu atoms and acetylene. [b] H(β). [c] H(α). [d] Calculated assuming a_H = 50 G. [e] Not resolved. [f] Reference 4. [g] Reference 5.

Table IV. ESR Parameters for the Vinyls Produced from Group 1B Metal Atoms and Some Disubstituted Acetylenes in Adamantane at 77 K

vinyl	a_M/G	g factor
$CuC[C(CH_3)_3]{=}\dot{C}C(CH_3)_3$	397	2.0007
cis-$CuC(C_6H_5){=}\dot{C}C_6H_5$	257	2.0005
trans-$CuC(C_6H_5){=}\dot{C}C_6H_5$	339	2.0012
cis-$AgC[C(CH_3)_3]{=}\dot{C}C(CH_3)_3$	−102.3	2.0004
trans-$AgC[C(CH_3)_3]{=}\dot{C}C(CH_3)_3$	~−150	
$AgC(C_6H_5){=}\dot{C}C_6H_5$	−108.3	2.0004
$AuC(C_6H_5){=}\dot{C}C_6H_5$	179	2.0054

SOMO in $M[C_2H_2]$.[3] The negative *g* shift for these complexes also indicates an appreciable contribution from an unfilled orbital to the SOMO.

The high metal s spin population is consistent with the ESR spectra of all the group 1B monosubstituted alkyne and disubstituted alkyne monoligand complexes. Unfortunately unpaired p orbital contributions could not be estimated because the spectra did not resolve to give $A_\parallel$ and $A_\perp$ contributions.

We have not undertaken ab initio calculations on the monocomplexes of these substituted alkynes, but the effects of substituents can be discussed qualitatively in terms of their effects on the energies of the π and π* levels and the tendency of the complexes to rearrange to the final adduct vinyl radical. Methyl substituents lower the π* level and raise the π level; the former reduces the π*–p separation while the latter reduces the π–d separation with a corresponding increase in stability of the complex. This is in accord with the experimental observation of the complexes $M[CH_3C{\equiv}CH]$ and $M[CH_3C{\equiv}CCH_3]$ for all three group 1B metal atoms. CF_3 substitution should have the opposite effects on the π and π* levels and hence lead to destabilization, again in agreement with the fact that no monoligand complexes are observed for the CF_3-substituted acetylenes. Phenyl-substituted alkynes should behave like the methyl-substituted alkynes, but in these cases no monoligand complexes are observed. This is probably not because the complexes are not formed but rather that they rearrange rapidly to form the resonance-stabilized vinyl radicals $C_6H_5\dot{C}{=}C(X)M$ (where X = H or C_6H_5). The absence of complexes for $(CH_3)_3C$-$C{\equiv}CH$ is difficult to explain since the *tert*-butyl group should have little effect on the π and π* levels. This is even more puzzling since the disubstituted alkyne $(CH_3)_3CC{\equiv}CC(CH_3)_3$ forms complexes. It is possible that the positive inductive and field effects of the *tert*-butyl group leads to an increased electron density at the nonsubstituted carbon and hence a propensity for the weakly electrophilic metal atoms to localize there; i.e., the formation of the vinyl is encouraged.

Substituted acetylenes give bis(alkyne) complexes with copper that are all more stable than the copper mono(alkyne) complexes and are observed even when the monoligand complex is not, e.g., $(CH_3)_3CC{\equiv}CH$, $CF_3C{\equiv}CH$, and $C_6H_5C{\equiv}CC_6H_5$. The values of the parameters $A_\perp(Cu) \approx 70$ G, $A_\parallel \approx 0$ G, and $A_\parallel(nH) = 30$ G are similar for all the complexes and are similar to the values reported by Kasai, McLeod, and Watanabe[3] for $Cu[C_2H_2]_2$. This suggests that most of these complexes are isostructural with $Cu[C_2H_2]_2$ which it has been concluded[3] has a planar D_{2h} structure with the Cu atom flanked by two parallel ligands.

A qualitative MO diagram based on our SCF calculation on the planar $Cu[C_2H_2]_2$ is displayed in Figure 8. The most striking difference between the bonding in the monoligand and diligand complexes is the character of the SOMO. In the case of $Cu[C_2H_2]_2$ strong interaction between the Cu $4p_x$ orbital and the π_y* orbital of the ligands pushes the energy of the latter orbital below the Cu 4s orbital. Therefore, the SOMO ($1b_{3u}$) consists of contributions from the Cu $4p_x$ and the ligands' antibonding orbitals and the ground state of $Cu[C_2H_2]_2$ has a $^2B_{3u}$ symmetry. This assignment lends theoretical support to the intuitive bonding scheme proposed by Kasai, McLeod, and Watanabe.[3] In Figure 9 we present the wave function contour diagrams for the molecular orbitals anticipated to be involved in strong bonding on the basis of the Dewar–Chatt–Duncanson model ($2a_g$, $1b_{2u}$, and $1b_{1g}$). It is clear from the wave functions that the nonbonding interaction between the filled Cu 3d and the ligands π orbitals is weak and that the sole contribution to the stability

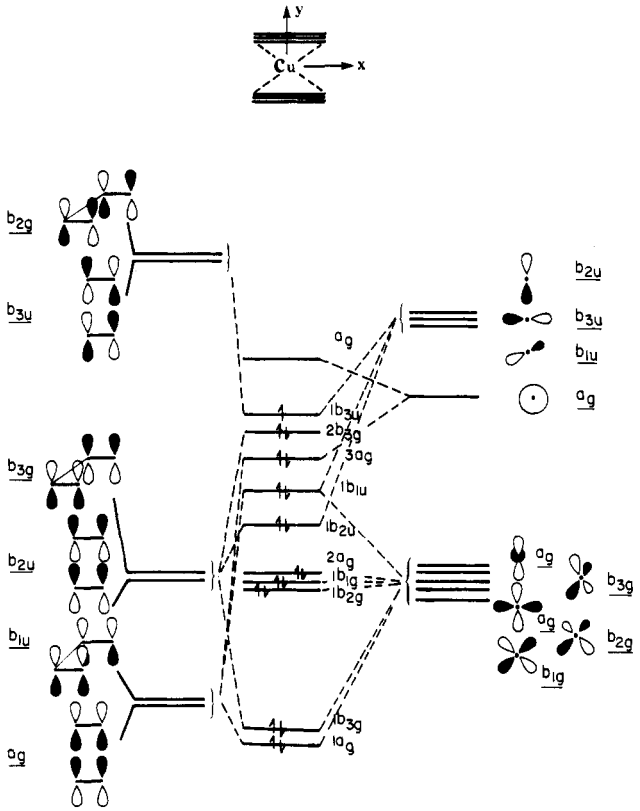

Figure 8. Schematic interaction diagram between Cu 3d, 4s, and 4p orbitals and ligand π orbitals in $Cu[C_2H_2]_2$.

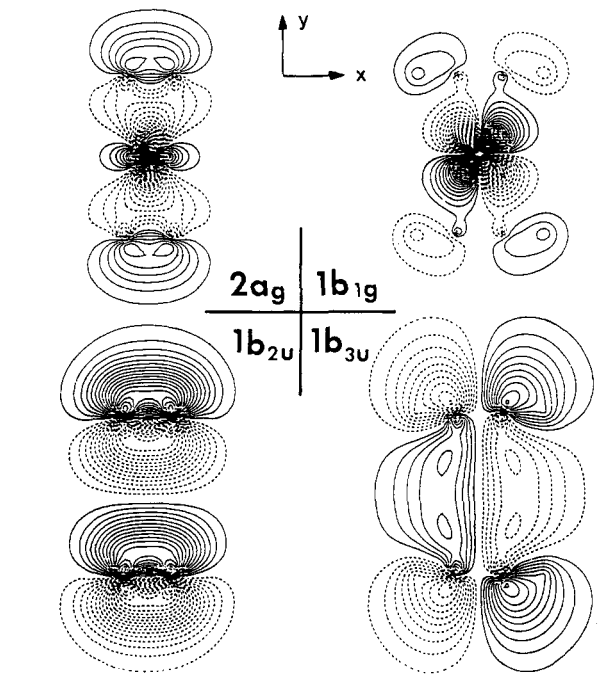

Figure 9. Wave function contour diagrams for the anticipated bonding molecular orbitals of $Cu[C_2H_2]_2$.

of the diligand complex arises from a strong interaction between the π_y* orbitals of the ligands with the Cu $4p_x$ orbital. The diffusiveness of the Cu $4p_x$ orbital results in better overlap with the acetylene π* orbitals.

It should, however, be noted that the Cu hyperfine interactions for copper bis(acetylene) complexes ($A_\perp >> A_\parallel$) are not entirely consistent with this description of the SOMO and suggest more d orbital participation. Furthermore the suggestion[5] that $Au[C_2H_4]_2$ is isostructural with a planar $Cu[C_2H_2]_2$ must be taken with some reservation because the former species has orthorhombic A and g tensors while the latter has axial and isotropic A and g tensors.

The enhanced stability of the copper and gold bis(alkyne) complexes probably arises because of a propitious matching of the metal valence p_x, p_y, d_{z^2}, and s orbital energies with the combinations of the π and π* orbitals of the acetylenes. The instability of the silver bis(alkyne) complexes may be associated with the much lower energy level of the metal 4d orbitals.

The ESR parameters for the adducts of group 1B metal atoms to monosubstituted acetylenes (Table III) show that copper adducts have metal hyperfine interactions from a high of 191.5 G for $CuCH{=}\dot{C}H$ to a low of 133.7 G for $CuCH{=}\dot{C}C_6H_5$. Comparison of a_{63} for $CuCH{=}\dot{C}H$ with the value for Cu atoms in adamantane[8] indicates a 4s spin population of 0.093. The β-hydrogen has an unpaired s spin population of 0.1, and the α-hydrogen hyperfine interaction is larger than the corresponding value for $CH_2{=}\dot{C}H$.[10] These results suggest that the geometry of $CuCH{=}\dot{C}H$ is different to that of $CH_2{=}\dot{C}H$ and $CuCH{=}\dot{C}C_6H_5$.[4] The metal hyperfine interactions for $CuCH{=}\dot{C}CH_3$ and $CuCH{=}\dot{C}CF_3$ fall between the values for $CuCH{=}\dot{C}H$ and $CuCH{=}\dot{C}C_6H_5$, suggesting that the angle between the orbital containing the unpaired electron and the C=C axis depends on the nature of the group attached to the α-carbon.

Interestingly Ag gives two adducts with $CH{\equiv}CC(CH_3)_3$ with silver hyperfine interactions of −110.5 and −149.6 G. The adducts to $CH{\equiv}CH$, $CH{\equiv}CCH_3$, and $CH{\equiv}CCF_3$ all give $a_{Ag} \approx -150$ G while $CH{\equiv}CC_6H_5$ gives $a_{Ag} = -109.6$ G. We are tempted to conclude from this data that the larger Ag hfi can be assigned to a vinyl with the Ag atom trans to the orbital containing the unpaired electron while the smaller Ag hfi can be assigned to a cis vinyl.

Au gives two radicals with $CH{\equiv}CC(CH_3)_3$ and $CH{\equiv}C\text{-}C_6H_5$ with the trans isomer having the larger Au hyperfine interaction. Reaction of Au atoms with monosubstituted acetylenes gives no indication of a vinyl–vinylidene rearrangement that is observed in the $Au\text{–}C_2H_2$ system.[4] There is, however, some circumstantial evidence for this rearrangement in the $Au\text{–}C_6H_5C{\equiv}CC_6H_5$ system.

The range of adducts produced by reaction of group 1B metal atoms with disubstituted acetylenes (Table IV) is not as large as it is with the monosubstituted acetylenes. The Cu adducts to $(CH_3)CC{\equiv}CC(CH_3)_3$ and $C_6H_5C{\equiv}C\text{-}C_6H_5$ do, however, have a_{Cu} significantly larger than the values for the monosubstituted acetylenes. Furthermore cis and trans stereoisomers appeared to be formed from diphenylacetylene.

It is worth noting that ground-state copper atoms form adducts with CH_3-, CF_3-, and C_6H_5-substituted acetylenes but not with acetylene itself (photoexcited Cu atoms in the ^2P state do form the adduct radical). The higher reactivity of the substituted acetylenes must arise from a lowering of the energy barrier because of the greater stability of radicals such as $CH_3\dot{C}{=}CHCu$ and $C_6H_5\dot{C}{=}CHCu$.

The formation of the carbon-centered radicals $\dot{C}H_2C{\equiv}CH$, $\dot{C}H_2C{\equiv}CCH_3$, and $\dot{C}F_2C{\equiv}CH$ is unexpected and could arise by a metathesis reaction of a single metal atom or could occur at the surface of nascent metal clusters and microcrystallites.

Acknowledgment. J.A.H. and B.M. thank NATO for a research grant. J.S.T. wishes to thank J.P. Daudey for permission to use his PSHONDO program package.

Registry No. $Cu[C_2H_2]$, 65881-80-3; $Cu[CH_3C{\equiv}CH]$, 89397-79-5; $Cu[CH_3C{\equiv}CCH_3]$, 89397-80-8; $Cu[(CH_3)_3CC{\equiv}CC(CH_3)_3]$, 89397-81-9; $Ag[CH_3C{\equiv}CH]$, 89397-82-0; $Ag[CH_3C{\equiv}CCH_3]$,

89397-83-1; Ag[$(CH_3)_3CC{\equiv}CC(CH_3)_3$], 89397-84-2; Ag[$C_6H_5C{\equiv}CC_6H_5$], 89397-85-3; Au[$CH_3C{\equiv}CH$], 89397-86-4; Au[$CH_3C{\equiv}CCH_3$], 89397-87-5; Cu[$C_2H_2]_2$, 65881-79-0; Cu[$CH_3C{\equiv}CH]_2$, 89397-88-6; Cu[$(CH_3)_3CC{\equiv}CH]_2$, 89397-89-7; Cu[$CF_3C{\equiv}CH]_2$, 89397-90-0; Cu[$CH_3C{\equiv}CCH_3]_2$, 89397-91-1; Cu[$(CH_3)_3CC{\equiv}CC(CH_3)_3]_2$, 89397-92-2; Cu[$C_6H_5C{\equiv}CC_6H_5]_2$, 89397-93-3; CuCH=CH, 89397-62-6; CuCH=$\dot{C}CH_3$, 89397-63-7; CuCH=$\dot{C}CF_3$, 89397-64-8; CuCH=$\dot{C}C_6H_5$, 84074-16-8; AgCH=$\dot{C}$H, 73373-74-7; AgCH=$\dot{C}CH_3$, 89397-65-9; *cis*-AgCH=$\dot{C}C(CH_3)_3$, 89397-66-0; *trans*-AgCH=$\dot{C}C(CH_3)_3$, 89397-67-1; AgCH=$\dot{C}CF_3$, 89397-68-2; AgCH=$\dot{C}C_6H_5$, 84074-17-9; AuCH=$\dot{C}$H, 84074-14-6; AuCH=$\dot{C}CH_3$, 89397-69-3; *cis*-AuCH=$\dot{C}C(CH_3)_3$, 89397-70-6; *trans*-AuCH=$\dot{C}C(CH_3)_3$, 89397-71-7; *cis*-AuCH=$\dot{C}C_6H_5$, 84074-19-1; *trans*-AuCH=$\dot{C}C_6H_5$, 84074-18-0; Cu[$C(CH_3)_3$]=$\dot{C}C(CH_3)_3$, 89397-72-8; *cis*-Cu$C(C_6H_5)$=$\dot{C}C_6H_5$, 89397-73-9; *trans*-Cu$C(C_6H_5)$=$\dot{C}C_6H_5$, 89397-74-0; *cis*-Ag$C[C(CH_3)_3]$=$\dot{C}C(CH_3)_3$, 89397-75-1; *trans*-Ag$C[C(CH_3)_3]$=$\dot{C}C(CH_3)_3$, 89397-76-2; Ag$C(C_6H_5)$=$\dot{C}C_6H_5$, 89397-77-3; Au$C(C_6H_5)$=$\dot{C}C_6H_5$, 89397-78-4; Cu, 7440-50-8; Au, 7440-57-5; Ag, 7440-22-4; $CH_3C{\equiv}CH$, 74-99-7; $(CH_3)_3CC{\equiv}CH$, 917-92-0; $CF_3C{\equiv}CH$, 661-54-1; $CH_3C{\equiv}CCH_3$, 503-17-3; $(CH_3)_3CC{\equiv}CC(CH_3)_3$, 17530-24-4; $CF_3C{\equiv}CCF_3$, 692-50-2; $C_6H_5C{\equiv}CC_6H_5$, 501-65-5; C_2H_2, 74-86-2.

Palladium(II)-Catalyzed Copolymerization of Carbon Monoxide with Ethylene. Direct Evidence for a Single Mode of Chain Growth[1]

Ta-Wang Lai and Ayusman Sen*

Chandlee Laboratory, Department of Chemistry, The Pennsylvania State University, University Park, Pennsylvania 16802

Received December 12, 1983

The series of cationic Pd(II) compounds $[Pd(PPh_3)_n(CH_3CN)_{4-n}](BF_4)_2$ (n = 1-3), which may be synthesized in situ or separately, were found to catalyze the copolymerization of CO and C_2H_4 at 25 °C and at a combined pressure of as low as 300 psi, in noncoordinating solvents such as $CHCl_3$ and CH_2Cl_2. Higher reaction temperatures were required in coordinating solvents, in the presence of excess PPh_3, or when more basic tertiary phosphines were used instead of PPh_3. The ethylene–carbon monoxide copolymer (E–CO copolymer) was a high melting solid having a regular structure with alternating carbon monoxide and ethylene units. The mechanism of the copolymerization is thought to involve a single mode of stepwise chain growth with alternate insertions of carbon monoxide and ethylene into a preformed Pd–alkyl bond. The intermediacy of Pd(II)–alkyl and –acyl species was supported by the observed catalytic activity of $Pd(PPh_3)_2(Me)(solv)^+$ and $Pd(PPh_3)_2(COMe)(solv)^+$. The use of alcohols as solvents for the copolymerization reaction resulted in the synthesis of polyketo esters of the type $RO(-COCH_2CH_2-)_nH$. Schultz–Flory plots of the oligomeric polyketo esters formed resulted in straight lines, supporting a stepwise chain growth mechanism. The rate of termination was found to decrease with increasing steric size and decreasing nucleophilicity of the alcohol used. The $\nu_{C=O}$ for the E–CO copolymer was abnormally low, and there was a monotonic decrease in $\nu_{C=O}$ with increasing n for the solid oligomeric polyketo esters. This was tentatively ascribed to the presence of intra- and intermolecular dipolar bonding between carbonyl groups.

The formation of polyketones through the copolymerization of CO with olefins is a reaction of significant practical importance. Because of the relative reactivity of the carbonyl group, these polyketones are expected to constitute a new class of photodegradable[2] and, perhaps, biodegradable polymers. In addition, because of the ease with which the carbonyl group can be chemically modified, such polyketones should be excellent starting materials for other, new types of functional polymers.[3]

Prior to our initial communication,[1] three basic methods for the copolymerization of CO with C_2H_4 were described in the literature[4-6] and their reaction conditions and the properties of the resultant ethylene–carbon monoxide copolymers (E–CO copolymers) are summarized in Table I. Only the palladium-catalyzed process yielded a regular alternating E–CO copolymer with CO/C_2H_4 ratio of 1. However, the reported procedures involved significantly elevated temperatures and pressures and, furthermore, no mechanistic information was available concerning this

Table I

	free radical initiated[4]	γ-radiation induced[5]	palladium catalyzed[6]
reaction conditions			
total pressure, psi	200-15 000	2100-2800	800-1900
temp, °C	120-165	25-90	95-135
product properties			
CO/C_2H_4	0.8-0.1	~1[b]	1
structure	random	variable	alternate
mp, °C	<25-117[a]	~180[b]	125-350
mol wt	280-7800	*c*	*c*

[a] Corresponds to copolymer of mol wt 1800.[4b] [b] Corresponds to a particular sample.[5b] [c] Not reported.

(1) Transition Metal Catalyzed Copolymerization of Carbon Monoxide with Olefins. 2. For part 1, see: Sen, A.; Lai, T.-W. *J. Am. Chem. Soc.* **1982**, *104*, 3520.

(2) (a) Heskins, M.; Guillet, J. E. *Macromolecules* **1970**, *3*, 224. (b) Hartley, G. H.; Guillet, J. E. *Ibid.* **1968**, *1*, 413. (c) Hartley, G. H.; Guillet, J. E. *Ibid.* **1968**, *1*, 165.

(3) For chemical modifications of the E–CO copolymer, see ref 4b and 5a.

(4) (a) Coffman, D. D.; Pinkney, P. S.; Wall, F. T.; Wood, W. H.; Young, H. S. *J. Am. Chem. Soc.* **1952**, *74*, 3391. (b) Brubaker, M. M.; Coffman, D. D.; Hoehn, H. H. *Ibid.* **1952**, *74*, 1509. (c) Brubaker, M. M. U.S. Patent 2 495 286, 1950.

(5) (a) Morishima, Y.; Takizawa, T.; Murahashi, S. *Eur. Polym. J.* **1973**, *9*, 669. (b) Chatani, Y.; Takizawa, T.; Murahashi, S.; Sakata, Y.; Nishimura, Y. *J. Polym. Sci.* **1961**, *55*, 811.

(6) (a) Nozaki, K. U.S. Patent 3 835 123, 1974. (b) Nozaki, K. U.S. Patent 3 694 412, 1972. (c) Nazaki, K. U.S. Patent 3 689 460, 1972. (d) Fenton, D. M. U.S. Patent 3 530 109, 1970.

0276-7333/84/2303-0866$01.50/0